An analysis of flow-simulation scales and seismic response

P. L. Stoffa, M. K. Sen and R. Seifoullaev, Institute for Geophysics; H. Klie, X. Gai, W. Bangerth, J. Rungamornrat and M. F. Wheeler, Center for Subsurface Modeling, The University of Texas at Austin.*

Summary:

Accurate integration of flow simulation and seismic modeling is one of the cornerstones of reliable time-lapse (4D) seismic monitoring. However, the question which scales flow simulations need to resolve to accurately capture reservoir changes during production and whether these scales are resolvable in seismic data is an open one. The answer impacts computational costs and our ability to predict reservoir changes from seismic observations. A sensitivity study is performed to determine the main seismic features due to pressure and saturation changes in an oil-gas reservoir during production. Numerical experiments show that saturation fronts can be effectively tracked at different flow and seismic resolution levels.

Introduction:

The issue of resolution of scales has been an active area of research in both reservoir engineering and geophysics; see e.g., Durlofsky (2003) and Sengupta and Mavko (2003). It has been primarily driven by the need to elucidate a clear threshold between computing time and achieving higher resolution and accuracy levels in the solution.

In spite of the fact that the current reservoir characterization tools can generate very refined reservoir models containing millions of gridblocks, it is still a major challenge to perform a flow simulation using such a fine grid. This has motivated the development of several upscaling techniques for running realistic simulations within a reasonable time. However, little has been reported on how the upscaling process should be linked or conditioned to the computation of seismic responses. Moreover, upscaling processes are generally followed by a downscaling step to generate a detailed representation of the impedance, velocity or stress field for seismic modeling. Downscaling is usually performed by linear interpolation between the values of neighboring grid blocks or Backus averaging.

Nevertheless, the problem of scale has been treated independently in both areas. The advent of time-lapse 4D seismic data processing brings new questions on how to calibrate resolution in flow and seismic simulations when the two processes are coupled in an iterative inversion procedure. At least two fundamental questions arise:

- What is the resolution required in fluid flow simulations to be able to capture the reservoir changes during production through seismic data?
- What is the resolution required in seismic data to be able to track the changes in the reservoir model and that make predictions in hydrocarbon production possible?

One would be tempted to say the higher the resolution the better. However, this may be prohibitively costly and time consuming with the resources available or impossible to achieve during data acquisition given current practice.

The methodology presented here shows that saturations are the key factor for tracking changes during production for an oil-gas reservoir. The reservoir changes are computed at different resolution levels and their corresponding seismic responses are analyzed using two seismic modeling techniques, a pure numerical approach (staggered grid explicit finite differences, Levander 1988) and a semi-analytic approach based on plane waves similar to the split-step Fourier migration method; see Stoffa et al. (1990).

Methodology:

We use a multi-physics, multi-scale flow reservoir model coupled with a petrophysical model described by Biot-Gassmann theory; Bourbie et al. (1987). The flow simulator is the Integrated Parallel Accurate Reservoir Simulator (IPARS) framework; a comprehensive description is provided in Wheeler and Peszynska (2002).

For the purpose of sensitivity analysis and determining the most relevant parameters affecting seismic velocities at different scales and simulation times, we use a simple argument from numerical analysis to compute the sensitivity associated with a given function. For the case of V_p depending on gas saturation, this number is computable from Biot-Gassmann's equations and is given by

$$\kappa_{S_g}(V_P) = \left| \frac{V_p(S_g)}{V_p(S_g)} S_g \right|. \qquad (1)$$

Analogous expressions can also be derived for V_p with respect to other phase saturations and pressure at different scales and flow simulation times. Figure 1 illustrates the sensitivity of $\kappa_{S_g}(V_p)$ with respect to V_p in an oil-gas reservoir. This plot illustrates the strong dependence that the seismic velocities show with respect to gas saturation fronts as demonstrated numerically in the next section.

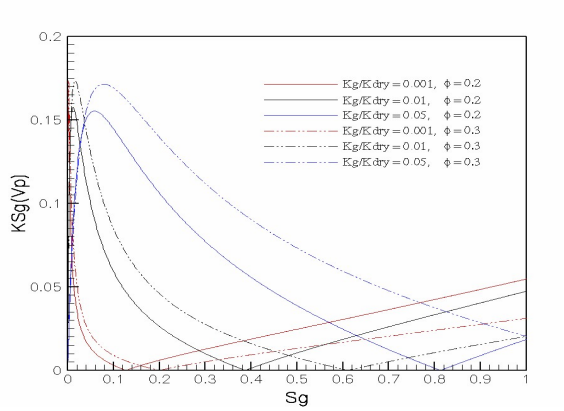

Figure 1. Sensitivity of P-wave velocities with respect to gas saturations in an oil-gas reservoir.

Based on these sensitivity considerations, we will in the following concentrate on the effects of changes in gas saturations on the seismic responses of the reservoir.

One aim of this study is to investigate the effects of resolved scales in the flow simulation. To this end, upscaling is performed in a static sense; i.e., flow responses would correspond to upscaling the permeability/ porosity heterogeneity, see Figure 2. The approach we follow is to successively apply wavelet transformations. Despite the fact that this may not be the most effective approach, it is simple, very efficient and reasonably powerful in capturing the main local features of the original data; see e.g., Sahimi et al. (2005). Also, static upscaling is the most popular technique used in the oil industry.

Numerical Experiments:

The numerical experiments were performed on model 1 of the SPE 10th Comparative Solution Project (see Christie and Blunt, 2001), describing a cross-sectional reservoir model that consists of 100x1x20 (fine) gridblocks in a regular Cartesian system. The size of each grid block is 25x25x2.5 ft^3. Two successive upscaled models were generated by halving the number of gridblocks along x and z; that is, of 50x1x10 (semi-coarse) and 25x1x5 (coarsest) gridblocks. The upscaling was performed using the Haar wavelet (Daubechies, 1992). The original model was slightly modified to allow oil and gas compressibility and capillary forces due to the interaction of these two phases. Figure 2 shows the resulting upscaled permeability fields in log scale. We notice that there are large lateral and vertical contrasts in this field (up to 4 orders of magnitude in several locations). A fixed production strategy was adopted with one gas injecting well located at the leftmost side of the model and a production well at the opposite extreme.

The flow simulation was carried out for 700 days (~1.9 years) at each grid resolution. As expected, the computation time was reduced by one order of magnitude for each reduction in grid resolution while nearly the same production curve was reproduced. The downscaled velocity and impedance fields were obtained with cubic spline interpolation to generate a smoother background compared to standard linear interpolation. Figure 3 shows the P-wave velocity profiles computed from the flow quantities using Biot-Gassmann's equations corresponding to each level of coarsening after 700 days of production.

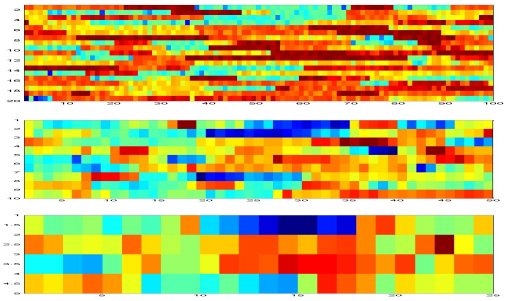

Figure 2. Upscaled permeability fields: 100x1x20 (top), 50x1x10 (middle), 25x1x5 (bottom).

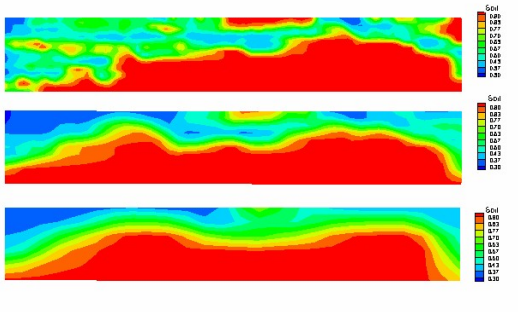

Figure 3. P-wave velocities after 700 days, fine grid (top), semi-coarse grid (middle), coarse grid (bottom).

All output models (46 time steps) from the IPARS runs were downscaled to 100x1x20 gridblocks of 2.5 ft and were converted to V_p, V_s, and density models for the seismic simulations. The resulting models were embedded into a background geologic model of dimensions 1200x1x1100. The edges of the embedded models were smoothed to better blend with the background model. For each time step of the flow simulation, both the elastic finite difference (FDPSV) and plane wave (PW3D) seismic forward modeling methods were used for all grid resolutions (fine, semi-coarse and coarse). Both methods were used for a high resolution (up to 400 Hz) and a more typical (up to 80 Hz) frequency range.

Plane wave modeling was carried out for a flat frequency response for ray parameters of 0.0 to 0.6 sec/km but only the results for the ray parameter equal to zero (normal

incidence case) is shown here. The plane wave responses were recorded at all 1200 horizontal grid positions (every 2.5 ft) at the top of the geologic model.

The finite difference modeling used a normalized derivative of a Gaussian with a peak frequency of 400 Hz as the source. The models were tapered at the sides and the top to reduce artificial reflections. For each production time step a single shot was acquired in the middle and at the top of the model. The responses were recorded at 590 receiver positions evenly distributed across the top of the model and spaced 5 ft apart.

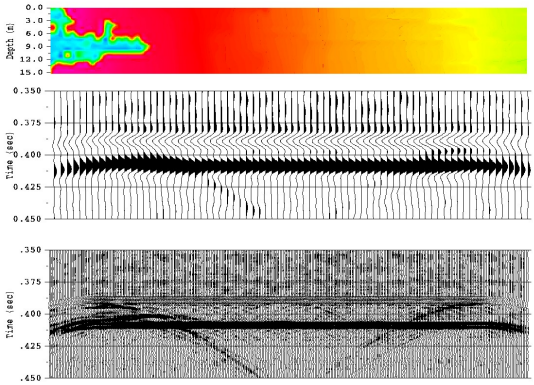

Figure 4. *P*-wave velocity (top), plane wave seismic profile at 80 Hz (middle) and 400 Hz (bottom) after 100 days

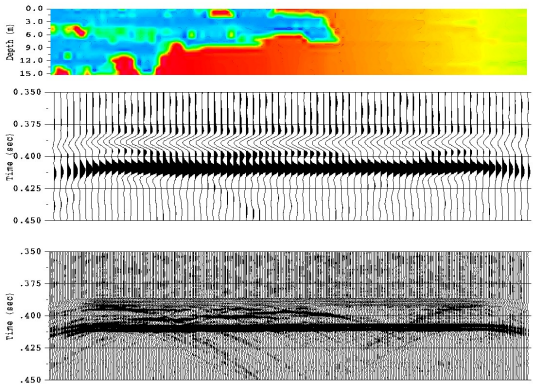

Figure 5. *P*-wave velocity (top), plane wave seismic profile at 80 Hz (middle) and 400 Hz (bottom) after 400 days.

Figures 4 to 7 show the results for the plane wave and finite difference modeling respectively for the finest reservoir grid after 100 and 400 days both at 80 Hz and 400 Hz. For the FDPSV modeling the hyperbolic events on the seismograms were flattened using a block-sum normal moveout. Between the snapshots at 100 and 400 days, changes are noticeable on the 80 Hz plane wave plots and in much more detail on the 400 Hz plane wave plots, while the changes for the finite differences, at both 80 Hz and 400 Hz, are present but much less noticeable.

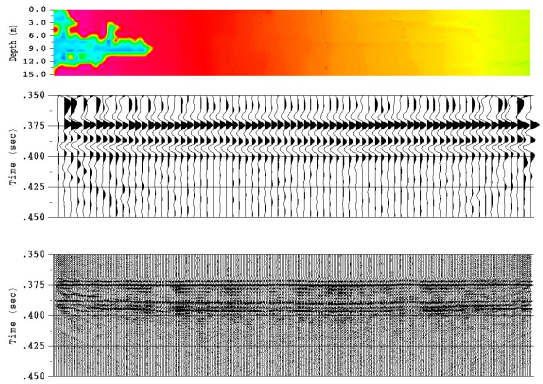

Figure 6. *P*-wave velocity (top), FDPSV seismic profile at 80 Hz (middle) and 400 Hz (bottom) after 100 days

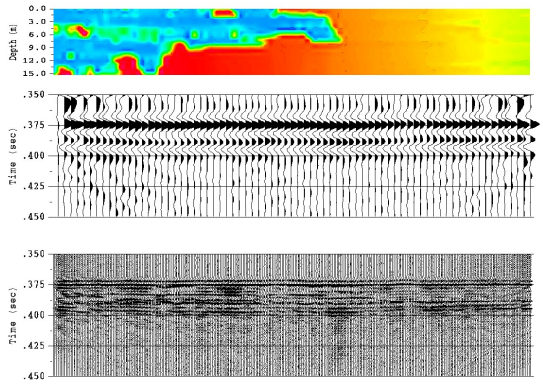

Figure 7. *P*-wave velocity (top), FDPSV seismic profile at 80 Hz (middle) and 400 Hz (bottom) after 400 days.

Figures 8 and 9 show the differences in the computed seismic responses for the reservoir grids for the 80 Hz plane wave seismic modeling at 400 days. Figure 8 is the seismic difference between the coarse and the fine reservoir grid and Figure 9 between the semi-coarse and fine reservoir grid. These plots are consistently scaled with a gain that is 10x greater than that used for the data in Figures 4-7. We see that there are observable differences, i.e., the seismic differences as displayed have significant amplitude. However, the seismic differences are also distinguishable when the two figures are compared. These are small indicating that the coarse resolution reservoir grid is probably acceptable at least for the initial seismic modeling/inversion tasks considering that typical seismic responses are generally less than or about 80 Hz. For the 400 Hz seismic models, Figure 10, there are changes

between the seismic differences (compare upper and lower seismic difference displays) for the coarse and semi-coarse reservoir grids as compared to the fine reservoir grid but again, these are modest except in a few locations.

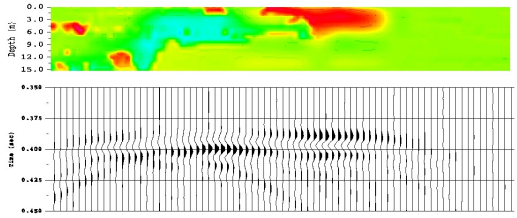

Figure 8. Differences in *P*-wave velocity (top) and plane wave seismic synthetics (bottom) at 80 Hz for the 400-day response between the coarse and fine reservoir grids.

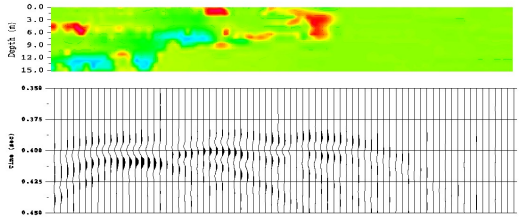

Figure 9. Differences in *P*-wave velocity (top) and plane wave seismic synthetics (bottom) at 80 Hz for the 400-day response between the mid and fine reservoir grids.

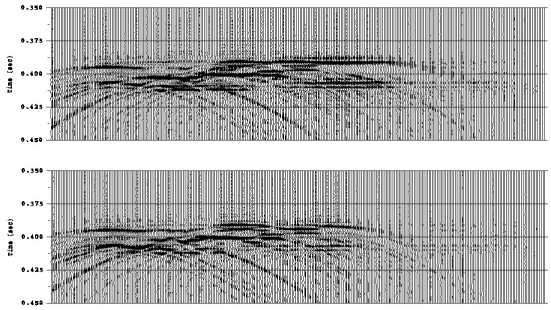

Figure 10. Differences in 400 Hz plane wave seismic synthetics at 400-days (top) between the coarse and fine reservoir grids and (bottom) between the mid and fine reservoir grids.

Conclusions:

To investigate the effect of scale used in reservoir simulation on seismic responses, we carried out a systematic numerical study using the 10th SPE reservoir model. The results from the flow simulation carried out at three reservoir grid resolutions were mapped into elastic models, which were used to generate synthetic seismograms. Our results indicate that at typical seismic frequencies the details of the reservoir model due to the effect of changes in saturation during production can definitely be noticed. Differences in the seismic responses due to differences in the reservoir simulation grid are small at 80 Hz (factor of 10 less than production time step seismic differences) but nonetheless observable.

References:

Bourbie, T., Coussy O. and Zinsner, B, 1987. Acoustics of Porous Media. IFP Publications.

Christie, M.A. and Blunt, M.J. 2001. Tenth SPE Comparative Solution Project: A Comparison of Upscaling Techniques: SPE Reservoir Simulation Symposium, Houston, Feb. 11-14. SPE 72469.

Daubechies, I., 1992. Ten Lectures on Wavelets. SIAM.

Durlofsky, L.J., 2003. Upscaling of Geocellular Models for Reservoir Flow Simulation: A Review of Recent Progress. 7th International Forum on Reservoir Simulation, Buhl/Baden-Baden, Germany, June 23-27.

Levander A.R., 1988. Fourth-order finite-difference P-SV seismograms, Geophysics, 53, 1425-1436.

Sahimi, M, Rasaei M.R, Ebrahimi, F and Haghighi, M., 2005. Upscaling of unstable miscible displacements and multiphase flows using multiresolution wavelet transformation. SPE Reservoir Simulation Symposium, Houston, TX, SPE 93320.

Sengupta, M and Mavko, G., 2003. Impact of flow-simulation parameters on saturation scales and seismic velocity, Geophysics, 68, No. 4, p. 1267-1280.

Stoffa, P.L., Fokkema J.T., de Luna Freire, R.M. and Kessinger, W.P., 1990. Split-step Fourier migration, Geophysics, 55, No. 4, 410-421.

Wheeler, M.F. and Peszynska, M., 2002. Computational Engineering And Science Methodologies For Modeling And Simulation Of Subsurface Applications. Advances in Water Resources, 25, pp.1147-1173.

Acknowledgements:

The authors want to thank the NSF for its support under the ITR grant EIA 0121523/EIA-0120934.